Modelling patient specific cardiopulmonary interactions

James Cushway[a,c], Liam Murphy[a], J. Geoffrey Chase[a],

Geoffrey M. Shaw[b] & Thomas Desaive[c]

August 11, 2025

[a]University of Canterbury, Department of Mechanical Engineering, Christchurch, New Zealand

[b]Dept of Intensive Care, Christchurch Hospital, Christchurch, New Zealand

[c]University of Liège (ULg), GIGA-Cardiovascular Sciences, Liège, Belgium

Keywords-Positive end-expiratory pressure, stressed blood volume, cardiovascular, cardio-pulmonary, thoracic pressure

Abstract

Mechanical ventilation is well known for having detrimental effects on the cardiovascular system, particularly when using high positive end-expiratory pressure. High positive end-expiratory pressure levels cause a decrease in stroke volume, which, under normal conditions, usually bring about a decrease in stressed blood volume. Stressed blood volume, defined as the total pressure generating volume of the cardiovascular system, has been shown to be a potential index of fluid responsiveness, making it a potentially important diagnostic tool. Generally, respiratory and haemodynamic care are provided independently of one another. However, that positive end-expiratory pressure alters both stroke volume and stressed blood volume suggests both the pulmonary and cardiovascular state should be conjointly optimised and used to guide positive end-expiratory pressure. However, the complex and patient-specific nature of cardiopulmonary interactions which occur during mechanical ventilation presents a challenge for accurate modelling of respiratory and cardiovascular interactions required to better optimise care. Previous models attempting to incorporate cardiopulmonary interactions have suffered from poor reliability at higher PEEP levels, largely due to an exaggerated effect of intrathoracic pressure on the cardiovascular system. A new parameter, alpha, is added to a previously validated cardiopulmonary model, to modulate the percentage of intrathoracic pressure applied to the vena cava and left ventricle. The new parameter aims to increase reliability under high PEEP conditions as well as provide a patient specific solution to modelling cardiopulmonary interactions. The results from the identified optimal alpha are compared to the original model to investigate how this new parameter may be used to create a more patient-specific cardiopulmonary model, which would be better suited for guidance of care in the ICU.

1 Introduction

Positive end-expiratory pressure (PEEP) is an important mechanical ventilation (MV) setting in the ICU. PEEP aims to improve alveolar recruitment and oxygenation [1–4]. Setting optimal PEEP is crucial for maximising alveolar recruitment and preventing ventilator induced lung injury (VILI) [5,6]. However, PEEP also creates a sustained positive intrathoracic pressure (ITP). The resultant cardiopulmonary interactions are highly complex and patient specific, presenting a large challenge in predicting overall cardiovascular response to changes in PEEP.

It is understood positive pressure ventilation decreases stroke volume (SV) and stressed blood volume (SBV) in the cardiovascular system (CVS) [7–9]. SBV is defined as the total pressure-generating blood volume in the circulation and describes the volume contributing to tissue perfusion. Recently, SBV has been shown to be a potential index of fluid responsiveness as it is a major determinant of the mean systemic filling pressure (MSFP) and thus, venous return, making it a potentially important diagnostic tool [10]

That PEEP alters both SV and SBV suggests both the pulmonary and cardiovascular state should be conjointly optimised and used to guide PEEP. Optimising these systems in isolation may benefit one system, but have highly detrimental effects on the other. A combined cardiopulmonary model has the potential to provide a better understanding of patient specific respiratory and cardiovascular state, as well as resulting cardiopulmonary interactions. This would enable simultaneous optimisation of all cardiovascular and pulmonary parameters.

Much study has gone into accurately modelling the CVS. Many of these are lumped models which aim to to trade off complexity for simplicity and identifiability [11–17]. Aside from lumped parameter models there are also many other ways to model the cardiovascular system [12, 18]. More detailed finite element models [19–21] offer far

greater resolution and detail, but are not identifiable to be personalised. Thus, for the personalised modelling analysis required to translate modelling to clinical use, lower order lumped parameter models are used in this work.

While the effects of the respiratory system on overall CVS dynamics are well studied and understood [22–25], exactly how, and to what extent, physiological properties of the heart and blood vessels within the thoracic chamber (TC) are affected remains unclear and patient specific. This lack of knowledge presents a challenge for accurate modelling of respiratory and cardiovascular interactions required to better optimise care [11, 12, 26]. Furthermore, cardiopulmonary interactions occurring during respiration are highly complex and affect large portions of the circulation.

Accurate modelling of all such effects would require a highly complex model, dependent on a very rich source of measurement data, not usually clinically available. Recent studies have attempted to model cardiopulmonary interactions by combining previously clinically validated respiratory and CVS models [14, 15]. The models are coupled by subjecting intrathoracic chambers, specifically the vena cava and left ventricle chamber, to ITP. The ITP causes a decrease in transmural pressure of the chambers, which affects both the flow and stressed blood volume of the system. However, the model uses a single chamber to represent the entire venous blood volume, removing the ability to differentiate between intra- and extra- thoracic veins. The result is a highly exaggerated effect on the venous blood volume from the exerted ITP, as the applied ITP decreases the stressed volume of the entire venous system. Indeed, de Bournonville *et al* [15] reported the model's reliability diminished with increasing PEEP.

It is common to observe increased PEEP levels in ICU. Thus, such a model would not be viable for model based care under these conditions. Further, the previously mentioned models use a fixed cardiopulmonary relationship, which would be applied to all patients across all conditions. The patient-specific nature of cardiopulmonary interactions requires a model with the capability to adjust to patient specific con-

ditions, as well as adapt to an evolving individual patient-specific condition. Such a model would be able to more accurately and reliably identify haemodynamic parameters, and would thus be better suited for model based care in the ICU.

This study thus aims to improve the reliability of the cardiopulmonary model at high PEEP levels, as well as the improve the model's ability to adapt to patient specific conditions, by use of an additional parameter to modulate the applied percentage of ITP transmitted to the vena cava and left ventricle. This parameter attempts to compensate for the lack of separation between intra- and extra- thoracic venous chambers by evenly distributing ITP over the whole venous blood system, thereby reducing the exaggerated effect of ITP on the system. The study uses haemodynamic and respiratory data from a preload reduction manoeuvre (RM) performed on 5 pigs with previously validated CVS and respiratory system models [5, 14–16, 27–31] to investigate the new parameter and how it effects model dynamics and errors, and ultimately evaluate whether the updated model is a potential candidate for model based care in the ICU.

2 Methods

2.1 Experimental Procedure

The experimental protocol was approved by the Ethics Committee for the use of animals at the University of Liege, Belgium between September - November, 2015 (Reference Number 14–1726). Five pure Pietrain pigs were anaesthetised and mechanically ventilated. Septic shock was then induced in the subjects via a single infusion of endotoxin (lipopolysaccharide from E. Coli, 0.5 mg/kg, infused over 30 min). Pre-endotoxin infusion, a 500 mL saline solution was administered over 30 min simulating fluid resuscitation therapy. Several PEEP driven recruitement manoeuvre (RMs) were performed on each pig both pre- and post- endotoxin. Aortic pressure in the subjects was continually measured via a catheter with a sampling rate of 250 Hz. Left ventricle pressure and volume were also continually measured at 250 Hz via an admittance pressure volume catheter inserted into the left ventricle via an apical stab.

2.2 Cardiovascular Model

The CVS model is a highly simplified lumped parameter model comprising of three Windkessel chambers representing the left ventricle, aorta and vena cava [13–16]. The chambers are connected by 3 flow resistances, which represent the output, input, and systemic resistance (R_o, R_i & R_s). Backward flow in and out of the left ventricle is prevented by input and output valves. The valves are modelled as diodes, which prevent flow across a negative pressure gradient. This simple model ensures theoretical identifiability and maximises practical identifiability [32], which elude more complex and detailed models [11, 12]. The model schematic is shown in Figure 1.

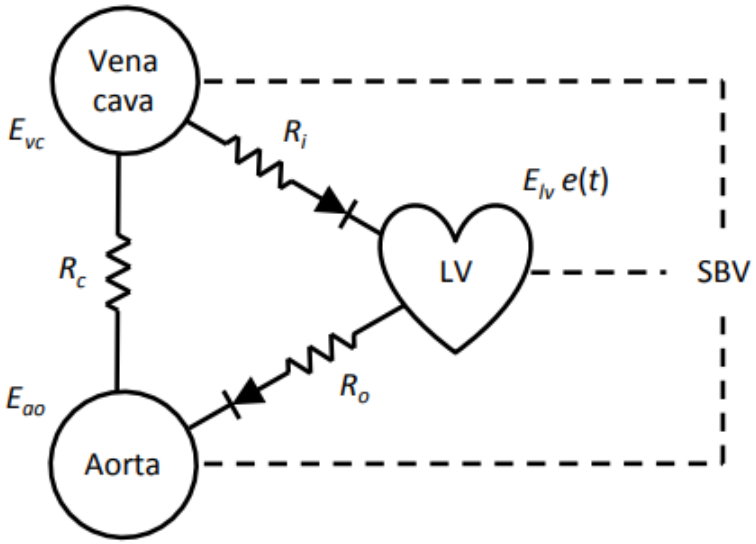

Figure 1: Three chamber CVS model

The aorta and vena cava are modelled as passive chambers, and thus their pressures are dependent solely on their stressed volume and elastance:

$$P_{ao}(t) = E_{ao}V_{sao} \tag{1}$$

$$P_{vc}(t) = E_{vc}V_{svc} \tag{2}$$

Where P_{ao}, E_{ao} and V_{sao} represent aortic pressure, elastance and stressed volume respectively and P_{vc}, E_{vc} and V_{svc} represent vena cava pressure, elastance and stressed volume, respectively.

The left ventricle uses time varying elastance [33] and is thus modelled:

$$P_{lv}(t) = e(t)E_{lv}V_{slv} \tag{3}$$

Where *e(t)* is the driver function creating time-variance. The driver function used in this work is taken from Davidson *et al* [34].

The flow into each of the chambers is modelled using Ohm's law. Systemic flow is thus defined:

$$Q_s(t) = \frac{P_a(t) - P_{vc}(t)}{R_s}. \tag{4}$$

The flows in and out of the heart are controlled by valves, and are thus represented using piecewise functions:

$$Q_o(t) = \begin{cases} \frac{P_{lv}(t) - P_{ao}(t)}{R_o} & P_{lv}(t) > P_{ao}(t) \\ 0 & \text{else} \end{cases} \tag{5}$$

$$Q_i(t) = \begin{cases} \frac{P_{vc}(t) - P_{lv}(t)}{R_i} & P_{vc}(t) > P_{lv}(t) \\ 0 & \text{else .} \end{cases} \tag{6}$$

The rate of change of stressed volume for each chamber is given by the difference of input and output flow:

$$\dot{V}_{sao}(t) = Q_o(t) - Q_s(t) \tag{7}$$

$$\dot{V}_{svc}(t) = Q_s(t) - Q_i(t) \tag{8}$$

$$\dot{V}_{slv}(t) = Q_i(t) - Q_o(t) \tag{9}$$

The CVS is a closed system and its total rate of change of volume is zero, yielding:

$$\dot{V}_{slv}(t) + \dot{V}_{sao}(t) + \dot{V}_{svc}(t) = 0 \tag{10}$$

Integrating Eq. 10 gives the constant stressed blood volume for the system, V_{s3}:

$$V_{s3} = V_{slv} + V_{sa} + V_{svc} \tag{11}$$

The model thus includes a total of 7 parameters; 3 elastances (E_a, E_{lv}, E_{vc}), 3 resistances (R_s, R_i, R_o) and the total stressed blood volume of the system, V_{s3}. Its simplicity enables its identifiability and potential clinical use [16, 32].

2.3 Respiratory System Model

The respiratory system model is a clinically validated lumped parameter model made up of a single Windkessel chamber to represent the lungs connected to a mechanical ventilator [5, 27–31]. The model schematic is shown in Figure 2.

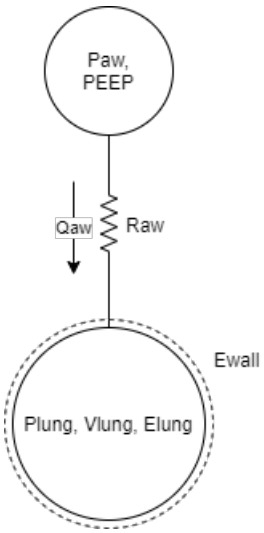

Figure 2: Single chamber respiratory system model

The respiratory system is connected to the ventilator via the airway resistance. Airway flow is defined using Ohm's law:

$$Q_{aw}(t) = \frac{P_{aw}(t) - P_{lung}(t)}{R_{aw}}, \tag{12}$$

where P_{aw} is the airway pressure supplied by the ventilator, P_{lung} is the lung pressure and R_{aw} is the airway resistance. The lung is a passive chamber, and the lung pressure can thus be defined:

$$P_{lung}(t) = E_{rs}V_{lung}(t) + PEEP \tag{13}$$

where V_{lung} is the lung air volume and E_{rs} is the respiratory system elastance, comprising of lung elastance, E_{lung}, and chest wall elastance, E_{wall}. Lung volume is determined by integrating airway flow:

$$V_{lung}(t) = \int Q_{aw}(t)dt + \frac{PEEP}{E_{rs}} \tag{14}$$

Airway flow and pressure, and lung volume are provided by the ventilator. Substituting Eq. 13 into Eq. 12 yields airway pressure [28]:

$$P_{aw}(t) = R_{aw}Q_{aw}(t) + E_{rs}V_{lung}(t) + PEEP \tag{15}$$

The two parameters of the system, R_{aw} and E_{rs}, are identified via multiple linear regression of measured ventilator data [14, 28].

2.4 Cardio-pulmonary Model Coupling

The models are coupled through thoracic pressure, as seen in Figure 3. Thoracic pressure is directly proportional to lung volume and the chest wall elastance:

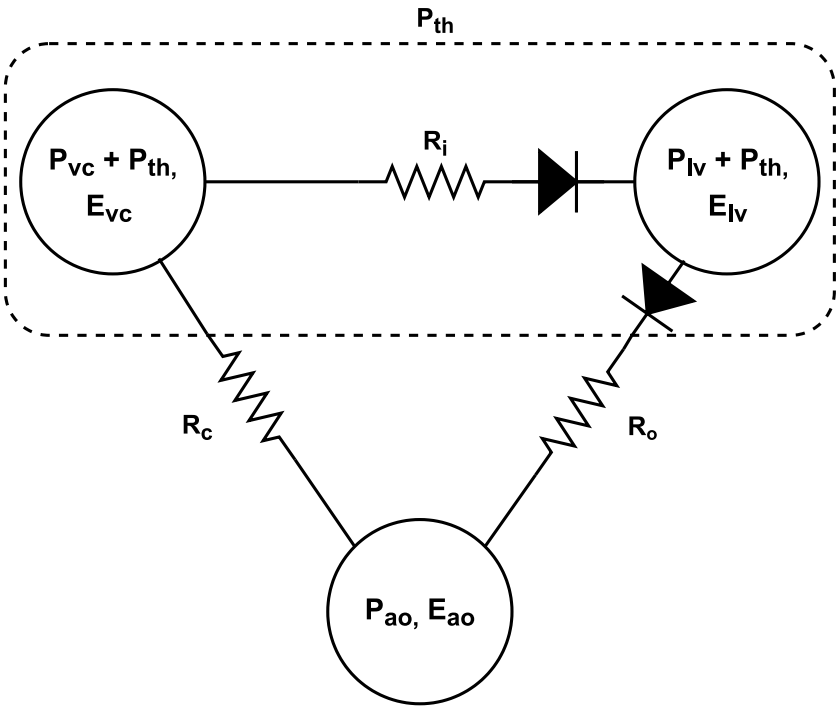

Figure 3: Coupled cardiopulmonary model. The thoracic cavity is represented by the dashed line and exerts intra-thoracic pressure, P_{th}, on the vena cava and left ventricle.

$$P_{th}(t) = E_{wall} V_{lung}(t) \tag{16}$$

where the chest wall elastance $E_{wall} = E_{rs} - E_{lung}$.

Substituting Eq. 14 into Eq. 16, thoracic pressure can be expressed:

$$P_{th}(t) = E_{wall} V_c(t) + PEEP \frac{E_{wall}}{E_{rs}} \tag{17}$$

Thoracic pressure acts to decrease the transmural pressure of vessels and chambers located within the TC. The stressed volume of a chamber is governed by transmural pressure [25, 35, 36]. The governing pressure volume relationship for an elastic chamber can thus be rewritten:

$$P_{tm}(t) = EV_s \tag{18}$$

Where $P_{tm}(t)$ is the transmural pressure of the chamber. Transmural pressure is the difference between interior and exterior chamber pressure, P_i and P_e. The equation can thus be rewritten:

$$P_i(t) - P_e(t) = EV_s \tag{19}$$

$$P_i(t) = EV_s + P_e(t) \tag{20}$$

By applying this relationship to vessels within the TC, namely the left ventricle and vena cava, their governing equations can be defined to include ITP:

$$P_{vc}(t) = E_{vc}V_{svc}(t) + P_{th}(t) \tag{21}$$

$$P_{lv}(t) = e(t)E_{lv}V_{slv}(t) + P_{th}(t) \tag{22}$$

This approach has been used by several models [14, 15, 17, 23].

However, while theoretically correct, an equation of such nature has several physiological implications. In particular, it posits ITP directly applies to haemodynamic pressures. However, this link is not direct, and occurs via interactions between blood flow in and around the lungs impacted by airway pressures changing vessel size, shape, and geometry.

In this model, since there is only one chamber to represent the whole venous system, the entirety of the venous system is subjected to ITP, whereas in reality, the majority of veins are extrathoracic and not subjected to ITP. As the venous system contains most of the volume of the circulation, such an assumption could have a highly

exaggerated effect on pressures and stressed volumes of the system, as the exerted ITP would cause both a large rise in intravenous pressure, and a large drop in venous SBV. Adding model complexity to rectify this situation creates model identifiability issues [11, 12, 16].

Indeed Debournonville *et al* reported as PEEP approached higher levels, the model became less reliable, and errors grew with increasing PEEP [15]. This issue is likely due to the excessive effect of ITP on the vena cava resulting in a large increase in model vena cava pressure, such an increase in vena cava pressure is not typically clinically observed with changing PEEP [37, 38]. Cushway *et al* did not observe an increase in model error as PEEP was increased [14]. However, there was no vena cava information used in the model, indicating vena cava pressure is indeed the source of error.

This problem could be solved by dividing the venous chamber into 2 separate chambers, an extra- and intra- thoracic chamber connected in series. However, since CVP is the only venous pressure measurement available in the ICU, there is no way to separate intra- and extra- thoracic venous chambers to better account for the effects of ITP and identify model parameters. Thus, the extent to which ITP exerts on the venous chamber must be adjusted to improve model reliability at high PEEP and prevent increasing model errors.

This goal can be most simply obtained by applying only a portion of ITP to the venous chamber:

$$P_{vc} = E_{vc}V_{svc}(t) + \alpha P_{th}(t) \tag{23}$$

where α represents the fraction of thoracic pressure transmitted to the vena cava. Furthermore, ITP applied to the left ventricle must also be adjusted, as a spatially heterogeneous ITP distribution would affect the pressure gradient for venous return:

$$P_{lv}(t) = e(t)E_{lv}V_{slv}(t) + \alpha P_{th}(t) \tag{24}$$

The process for finding α is described in the parameter identification section.

The final coupled model includes 10 cardiopulmonary parameters from the CVS and respiratory system models [5, 14–16, 27–31], as well as α for adjusting applied ITP.

2.5 Nominal Parameters and Subset Selection

Where possible, nominal parameters are estimated from measurement data. Where data was unavailable, values are obtained from the literature. The nominal parameters are summarised in Table 1.

Table 1: Parameter definitions

Parameter	Parameter Definition
E_a	$\frac{\Delta P_a(t)}{CO.T}$ [15]
E_{lv}	$max_T \frac{P_{lv}(t)}{V_{lv}(t)}$ [16]
E_{vc}	$\frac{\Delta P_{vc}(t)}{CO.T}$ [15]
R_c	$\frac{\overline{P}_a(t) - \overline{P}_{vc}(t)}{CO}$ [16]
R_i	$\int_{P_{vc}(t) > P_{lv}(t)} (P_{vc}(t) - P_{lv}(t))dt$ [16]
R_o	$0.04 mmHg.s/ml$ [16]
$V_{s,3}$	$\overline{V}_{lv}(t) + \frac{\overline{P}_a(t)}{E_a} + \frac{\overline{P}_{vc}(t)}{E_{vc}}$ [16]
E_{wall}	$\frac{E_{rs}}{2}$ [7]

To ensure structural and practical identifiability [32, 39], a subset of sensitive parameters was chosen for optimisation for all pigs. Sensitivity and correlation analyses per the method in [40] were used to identify a subset of parameters which could be reliably identified from the measurement data.

2.6 Output vector and parameter identification

Model outputs were chosen as clinically relevant beat-to-beat metrics, rather than time dependent measurements. This choice is largely due to the fact the temporal evolution of all signals is not always available or exportable from bedside machines [40,41]. As such, only beat-to-beat data, such as mean pressures and pulse pressures, are assumed to be available, where these values are also clinically used over the waveforms themselves.

Outputs were chosen to ensure structural identifiablility [32, 39, 42, 43]. The work by Pironet lists the model outputs required to ensure structural identifiablility of the CVS model [16, 40]. Furthermore, to quantify the ability to incorporate cardiopulmonary interactions, the change in aortic peak pressure over the course of a respiratory period is used [14, 15]. Thus, the output vector is defined:

$$X_{output} = [\overline{P}_a(t),\ \Delta P_a(t),\ \overline{P}_{vc}(t),\ \Delta P_{vc}(t),\ \overline{V}_h(t),\ SV, \Delta max(P_a(t))] \tag{25}$$

2.6.1 Error Function

The error function is a measure of accuracy for identified model outputs. If y^{ref} is a vector containing the N_y reference measurements and $y(p)$ is the output vector of parameter vector, p, each output's error is defined as the difference between the measurement and the output:

$$e_i(p) = y_i^{ref} - y_i(p),\ i \in [1, N_y] \tag{26}$$

The error function is then defined using the RMS of all errors:

$$\psi(p) = \sqrt{\frac{\sum_{i=1}^{N_y} e_i(p)^2}{N_y}} \tag{27}$$

2.6.2 Parameter Identification

The parameter identification in this work was performed using MATLAB's (The Mathworks, Natick, MA, USA) *fmincon* function. The parameter subset and error function were passed as parameters. Parameter estimation was performed for all 3 pigs over the first and last 5 beats for each PEEP level of the RM.

To find α, the parameter identification process was repeated for $\alpha \in \{0, 0.1...1.0\}$. The value for α resulting in the lowest error was selected for each pig. This sensitivity analysis and parametric optimisation over α seeks to find the appropriate fraction of ITP transmitted and assesses how pig specific it is.

2.7 Analysis and Comparisons

Model dynamics and quality of fit were analysed by checking the mean absolute error (MAE) of parameter estimates and by comparison of simulated and measured waveforms. To investigate the effects of thoracic pressure of each model, vena cava and diastolic left ventricle pressure outputs are compared to measurement equivalents. Furthermore, calculated thoracic pressure is plotted alongside measurement diastolic pressure to compare the increase of thoracic pressure against the measurement diastolic pressure as PEEP is increased.

3 Results

3.1 Experimental Results

The measurements from the RM are shown in Figures 4 and 5. Figure 4 shows the evolution of SV over the course of the RM. Figure 5 shows the left ventricle, aortic and vena cava pressure measurements over the course of the RM.

As expected, SV decreases over the course of the RM for all pigs. All pigs showed a substantial decrease in left ventricular pressure as well. However, some pigs were affected far more severely than others. Pigs 4 and 5 show much smaller decreases, 16.1±2.5% and 15.9±1.2% respectively, when compared to the decreases in Pigs 2 and 3, 31.5±1.3% and 36.3±2.0% respectively, illustrating the patient specific nature of cardiopulmonary interactions. Unlike systolic pressure, vena cava pressure and left ventricle diastolic pressure remain largely unchanged throughout the course of the RM for all pigs.

3.2 Parameter Subset Selection

The 2 least sensitive parameters for all pigs were the input and output resistances, R_i&R_o. They were omitted from the final parameter subset. The final parameter subset was thus defined:

$$P = [E_{ao},\, E_{lv},\, E_{vc},\, R_s,\, V_{s,3}] \tag{28}$$

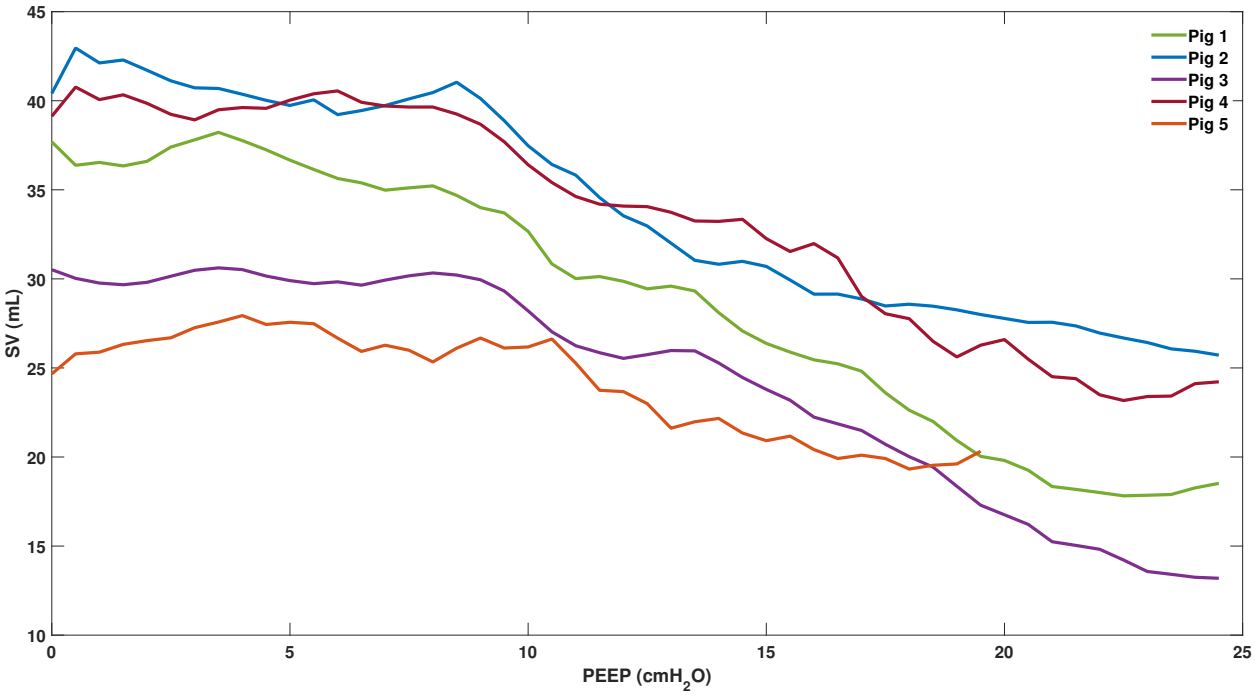

Figure 4: Stroke volume for each pig over the course of the RM. The green, blue, purple, red and orange lines represent Pigs 1, 2, 3, 4 and 5 respectively.

3.3 Optimal α

The optimum α was selected as the value minimising the MAE of the error vector for the model. Figure 6 shows MAE vs α of each pig for PEEP levels 10, 15 and $20 cmH_2O$. As α is incremented from 0, MAE decreases until an optimum value is reached, following which the error begins increasing again. Not only do optimum α values differ between pigs, but also between different PEEP levels of the same pig. This highlights not only the patient specific nature of cardiopulmonary interactions, but also the model's potential ability to adapt to these differing conditions.

As can be seen in Figure 6, the optimum value of α changes with PEEP for each pig. Figure 7 shows the optimum alpha of each PEEP level for each pig. As PEEP is increased, optimum α tends to decrease as expected, since the higher PEEP levels lead to higher ITP, which has a greater effect on vena cava pressure. A lower value α results in lower applied ITP, which has a lesser effect on vena cava pressure and its

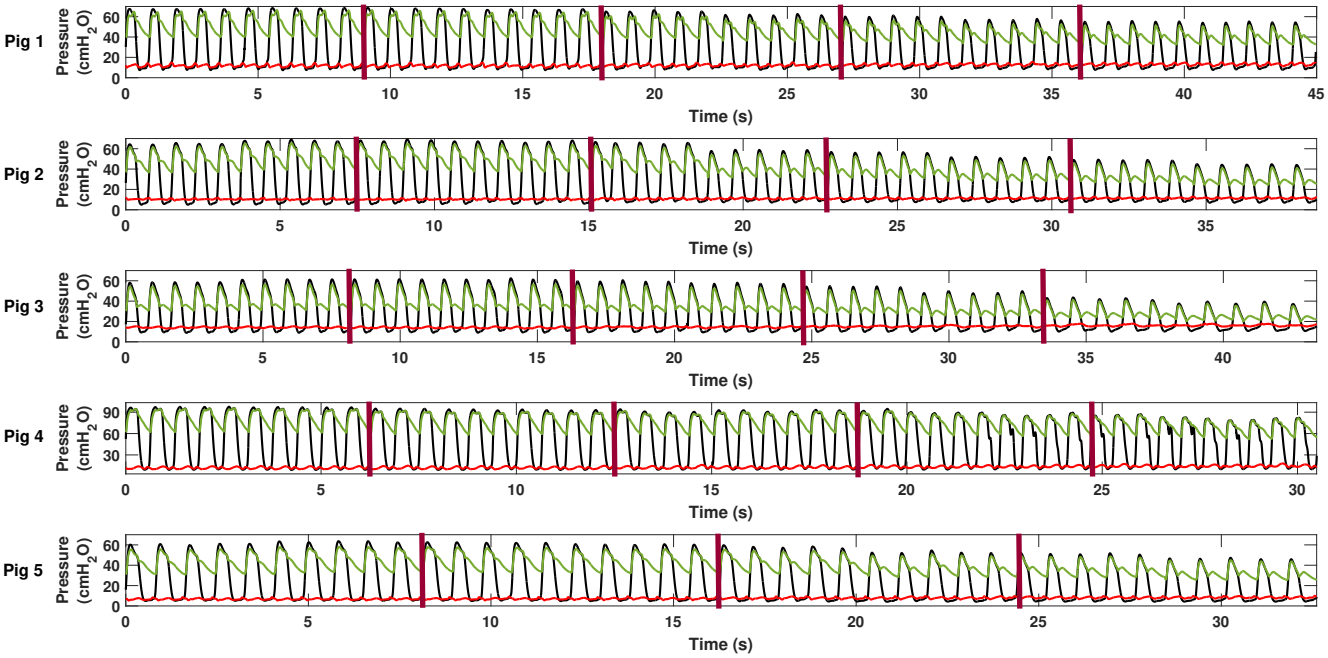

Figure 5: Pressure measurements for each pig over the course of the RM. Left ventricle, aortic and vena cava pressure are represented by the black, green and red line respectively while rows 1, 2, 3, 4 and 5 show the results for pigs 1, 2, 3, 4 and 5 respectively. PEEP changes are represented by vertical red lines, where PEEP is increased from $0cmH_2O$ in $5cmH_2O$ increments.

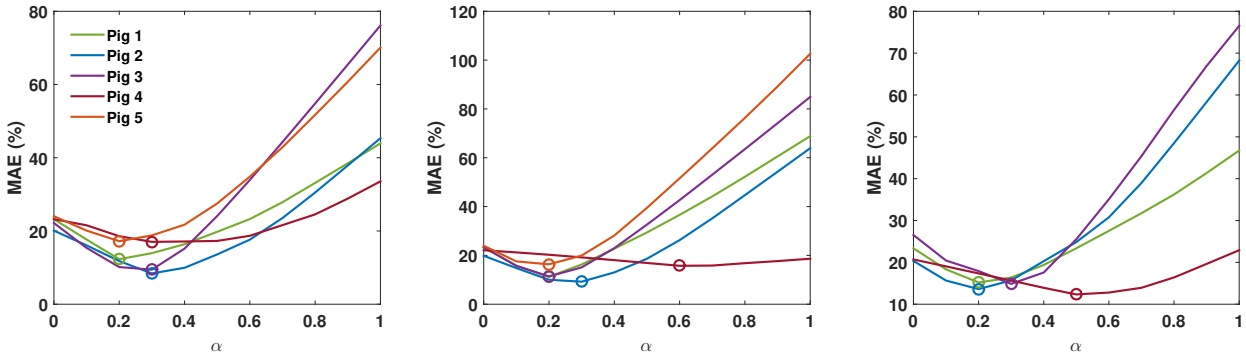

Figure 6: MAE vs alpha for each pig at PEEP = 10, 15 and 20 cmH_2O (left, middle and right respectively). The green, blue, purple, red and orange lines represent Pigs 1, 2, 3, 4 and 5 respectively. Optimal values for α are marked with dots.

stressed volume. Consequently, with lower α, the model is better able to reproduce vena cava pressure.

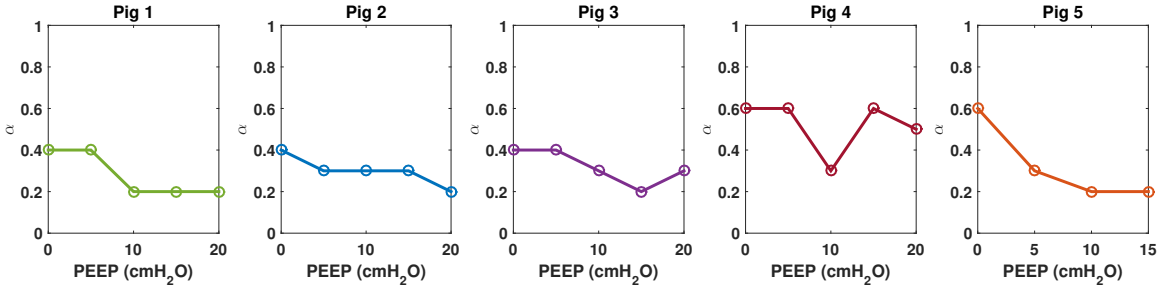

Figure 7: Optimum α vs PEEP for each pig.

The value of α also has a direct effect on left ventricle pulse pressure. However, the error does not use left ventricular pressure metrics as it is not available in a clinical setting. Nevertheless, the effect of α on left ventricular pressure can still be illustrated by comparing model left ventricular pulse pressure to experimental measurements. The pulse pressure error for each pig over all α values throughout the course of the RM is shown in Figure 8. As alpha increases from 0 to 1, left ventricular pulse pressure error increases with alpha. As vena cava pressure rises due to ITP, so too must left ventricle diastolic pressure. If diastolic pressure did not rise, vena cava pressure would surpass diastolic pressure, preventing blood from returning to the ventricle.

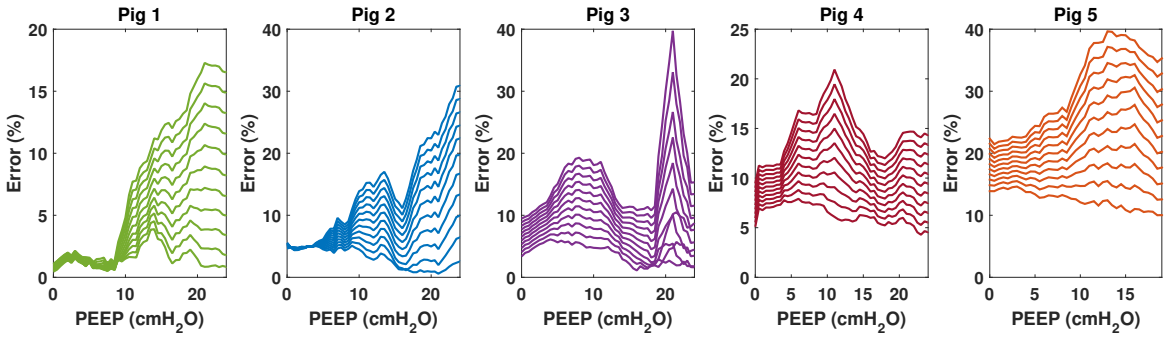

Figure 8: Pulse pressure errors for each pig over all alpha values during the RM. The green, blue, purple, red and orange lines represent Pigs 1, 2, 3, 4 and 5 respectively. Each error contour represents a value of alpha, with the lowest contour representing $\alpha = 0$ and the highest representing $\alpha = 1$.

3.4 Model Outputs

Model outputs were plotted alongside measured data to visually analyse model accuracy and the effect of thoracic pressure in both the α =optimum and $\alpha = 1.0$ models, where $\alpha = 1$ is the typical assumption [14, 15, 17]. The left ventricle and vena cava pressure measurements and model outputs are shown in Figure 9. The first and last 3 beats of each PEEP section are combined to form a continuous wave.

The left ventricle diastolic pressure and vena cava pressure for $\alpha = 1.0$ vary significantly when contrasted to the measured data, clearly demonstrating the exaggerated effect of ITP on the left ventricle and vena cava. However, the model with optimum α displays much stabler pressure measurements and closer resembles the measurement data. This illustrates how α is able improve model accuracy and reliability under increasing PEEP. The magnified diastolic pressure is shown in Figure 10.

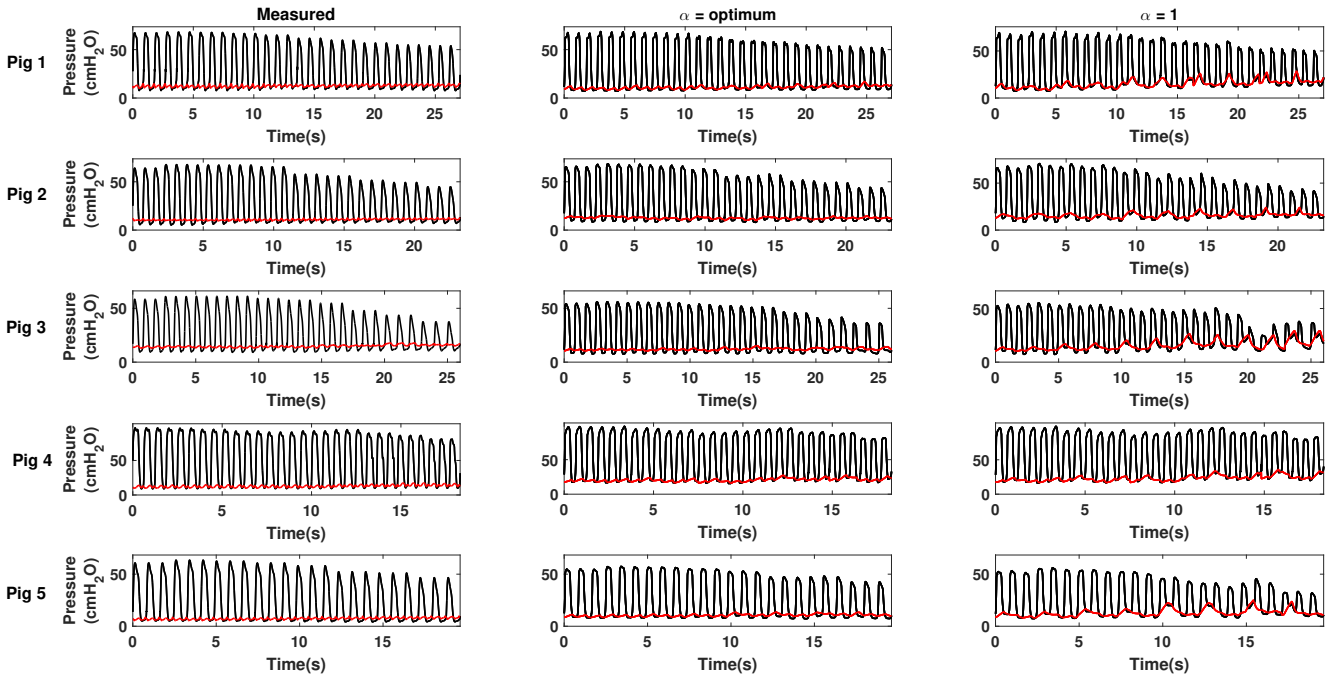

Figure 9: Left ventricle and vena cava pressure measurements and model outputs. Left ventricle pressure is shown in black while vena cava pressure is shown in red. Rows 1, 2 and 3 represent Pigs 1, 2 and 3 respectively while columns 1, 2 and 3 represent measured data, optimum α and $\alpha = 1.0$ models respectively.

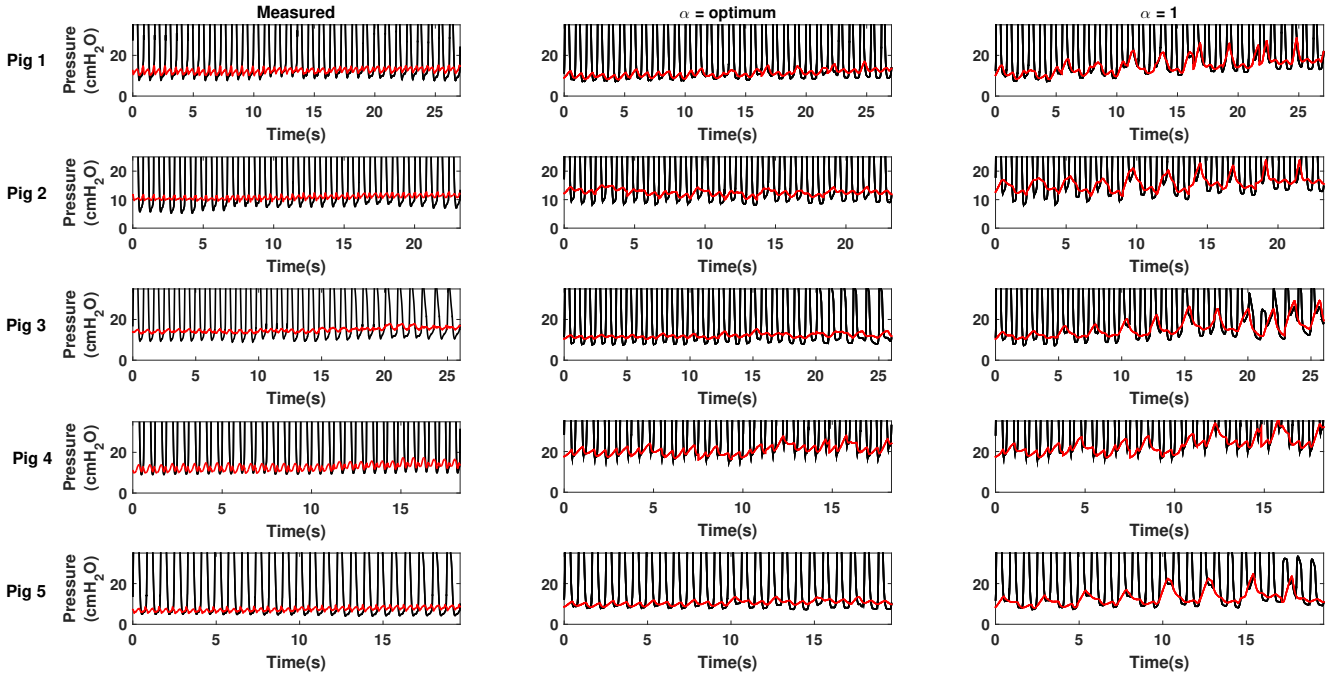

Figure 10: Diastolic left ventricle and vena cava pressure measurements and model outputs. Left ventricle pressure is shown in black while vena cava pressure is shown in red. Rows 1, 2 and 3 represent Pigs 1, 2 and 3 respectively while columns 1, 2 and 3 represent measured data, optimum α and $\alpha = 1.0$ models respectively.

4 Discussion

4.1 Effect of MV on the CVS

It is well known MV usually brings about a decrease in SV [14,25,29,36,44,45]. However, the extent to which SV is affected, and the exact effects which bring about this decrease are not clearly understood. Cardiovascular effects caused by mechanical ventilation are highly dependent on both the pulmonary and cardiovascular state of the patient, creating a large challenge for both clinicians and those attempting to model the CVS.

To optimise care and improve modelling, it is important to obtain a simultaneous understanding of the effects of MV on the CVS and the patient-specific cardiopulmonary state. MV affects both the right and left circulation. However, since the right circulation lies entirely within the TC and much of the left circulation lies outside of the TC, the two circulations are affected very differently. While the effects on the 2 circulations are not independent, it is important to distinguish between them.

4.1.1 Effect of MV on the right circulation

Since the the right circulation is located exclusively within the TC, ITP should act largely equally on all parts of the circuit, and thus, does not alter pressure gradients of the system [36,45,46]. However, The volume of blood within a vessel is dependent on its transmural pressure [35, 36]. As ITP increases, the external pressure acting on the vessels of the right circulation increases, causing a decrease in transmural pressure, thus decreasing vessel volume. This decrease in volume of the vessels and chambers of the right circulation leads to an initial increase in flow to the left ventricle, thereby displacing blood volume from the right to left circulation [36, 47].

Increasing PEEP causes the lungs to expand, recruiting previously collapsed alveoli and further distending those already recruited. As alveoli are recruited, lung volume increases, and previously hypoxic vasoconstricted vessels are supplied with oxygenated blood and resume normal function, decreasing vessel resistance and potentially reducing total pulmonary vascular resistance (PVR) [46, 48]. Conversely, as the alveoli expand and lung volume increases, alveolar capillaries are compressed and stressed, increasing their resistance and elastance.

Thus, the resultant effect on PVR due to lung expansion is difficult to predict. Patients with lung disease may experience an overall decrease in pulmonary resistance, as the decrease in resistance caused by providing oxygenated blood to hypoxic vasoconstricted vessels outweighs the increase due to vessel compression. Patients operating in a normal range will generally experience an increase in PVR. However, the extent of these net effects is highly unpredictable [48].

The expansion of the lungs also augments ITP, thereby increasing external pressure acting on intrathoracic vessels. Blood flow through vessels is dependent on the pressure gradient across them, the resistance and elastance of the vessel, and, importantly, the external pressure of the vessel [35, 36, 47]. An increased external pressure on a vessel causes it to become stiffer, increasing its resistance and elastance respectively. If external pressure remains lower than internal pressure, the vessel remains fully open and the effect on resistance is negligible. However, if the external pressure exceeds the internal pressure of the vessel, vessel walls may partly collapse and resistance to flow increases significantly [35]. Furthermore, if the external pressure increases until it exceeds vessel output pressure, but not vessel input pressure, the pressure gradient governing flow through the vessel now becomes the gradient of input pressure and vessel external pressure, reducing the pressure gradient, thereby decreasing flow through the vessel [36].

The change in both vessel resistance and vessel flow from increasing PEEP is thus highly dependent not only on ITP, but the ITP relative to the vessel pressure,

which change with patients, condition, and as condition evolves. Furthermore, ITP changes due to increasing PEEP are proportional to lung compliance [5, 14, 47–49]. Consequently, stiffer lungs result in lower ITP while more compliant lungs result in a higher ITP for a given PEEP, resulting in very different changes in end expiratory lung volume based on lung recruitability [49, 50]. The change in vessel resistance and flow is thus also dependent on lung compliance and overall pulmonary state.

Furthermore, the vena cava is also located within the TC, and like the vessels of the pulmonary circulation, the ITP exerted on the vena cava causes an increase in both its resistance and elastance, potentially reducing blood flow from the vena cava to the right atrium, thus reducing venous return. If ITP exceeds vena cava pressure, it would cause the walls of the vena cava to collapse [35, 36], further increasing resistance to flow and reducing return to the right atrium. The reduced flow to the right atrium decreases the preload of the right ventricle, further impacting its SV and return to the left heart. The extent to which resistance to venous return is affected thus depends on whether ITP exceeds vena cava pressure or not.

4.1.2 Effect of ITP on the left circulation

Unlike the right circulation, only part of the left circulation lies in the TC and thus ITP effects the pressure gradients of the circuit. The left ventricle lies within the TC, while most of the aorta and downstream arteries lie outside. The increase in ITP decreases the transmural pressure of the left ventricle, thereby increasing the pressure gradient between the left ventricle and the downstream extrathoracic aorta, resulting in a lower left ventricle afterload [25, 46–48, 51]. Furthermore, as discussed previously, the initial effects of ITP displaces blood from the pulmonary to systemic circulation, resulting in an initially increased blood flow to the left ventricle. The increased flow and decreased afterload result in an initial increase in left ventricle stroke volume.

However, as venous return to the right ventricle diminishes, and its afterload increases due to increasing PVR, the venous return to the left ventricle is also reduced, causing a reduction in preload, ultimately leading to a decrease in SV. The reduced filling volume results in a reduced preload, which results in a reduction of both SV and end systolic pressure. This in turn causes a decrease in the mean and pulse pressure of the aorta and all downstream arteries. Conversely, patients suffering from certain left ventricular disorders, such as hypervolemic or congestive heart failure, may actually experience a lasting increase in SV from the decreased afterload [46, 47]. However, this effect is limited by the diminishing return from the RV. The resultant effect on SV in such patients is harder to predict as there is no way of knowing at which point decreasing return begins offsetting the augmented ejection.

It is important to note all the above mentioned effects are patient specific and depend on a patient having both healthy circulatory and respiratory systems operating within standard parameter ranges. Patients with disease or weakened cardiovascular systems may experience more severe reactions to ITP caused by positive pressure ventilation. Patients with right ventricular dysfunction, commonly encountered in ARDS, are at potential risk of right ventricular failure due to the increased strain caused from the increased afterload [52, 53]. Right ventricular dysfunction is also reported to be one of the major determinants of mortality in ARDS [53]. Furthermore, the above-mentioned effects of ITP do not take into account the complexities of the autonomic nervous system responsible for ensuring proper circulatory function. While the effects of ITP on a fixed system are somewhat easy to comprehend, the difficulty of task is greatly magnified when considering the many compensatory mechanisms present within the CVS, which themselves are also patient specific and highly dependent on the health of the patient [25].

4.2 Experimental results

During the RM, all pigs displayed similar trends. Most notably, both SV and left ventricle pulse pressure decreased with increasing PEEP. All pigs showed a decrease in SV and left ventricle pulse pressure. However, pulse pressure of Pigs 2 and 3 remained more stable than those of Pigs 4 and 5, illustrating the patient specific nature of the cardiopulmonary effects. Additionally, despite having one of the largest reductions in left ventricle pulse pressure, 31.5±1.3%, Pig 2 had one of the smallest reductions in SV (32.7±3.0%). Pigs 1 and 5 had the largest reductions in SV, 50.0±2.4% and 50.9±4.4% respectively, despite very large differences in the reduction of their left ventricle pulse pressure, 21.3±1.2% and 36.3±2.0% respectively, further emphasising the patient specific nature of haemodynamic reactions to MV. Both mean and pulse aortic pressure also decreased for all pigs. Both left ventricular diastolic pressure and vena cava pressure remained fairly constant throughout the RM for all pigs, increasing very slightly with each PEEP step as expected. These results highlight the fact all pigs behaved as clinically expected overall, but with a wide level of inter-subject variability and specificity in response.

Further, the pigs all display different changes between PEEP levels. The increment from $0cmH_2O$ to $5cmH_2O$ does not appear to have much affect on any of the haemodynamics of the pigs, some pigs even appear to display an increase in left ventricle pulse pressure. Pig 3 has a much larger decrease in left ventricular pulse pressure when PEEP is increase from 15 to $20cmH_2O$ compared to the PEEP increment from 10 to $15cmH_2O$, 28.8±1.5% and 10.9±1.9% respectively, whereas Pig 1's decrease over the same increments are the same, 8.5±0.8% and 0.87±0.6% respectively. Clearly, it would be very difficult to create any fixed cardiopulmonary relationship applicable to all pigs, across all PEEP levels, given the large differences observed between the responses of each pig, and between the responses observed for changes in PEEP for a given pig.

4.3 Alpha selection

The optimum α value resulted in the lowest model error. As α increased, error decreased as cardiopulmonary interactions were better modelled. However, at a certain value, the errors grew as ITP began to have an increasingly exaggerated effect on the model, producing inaccurate model vena cava and left ventricle diastolic pressure.

As α is increased from $\alpha = 0.0$, the no interaction case, the model is able to account for cardiopulmonary interactions by exerting ITP on the vena cava and left ventricle, and overall model error decreases. When α is too low, the model is able to produce accurate outputs, but cannot reproduce the pressure fluctuations seen over the course of a respiratory period. As a result, there is a higher error in Δ aortic peak pressure over each respiratory cycle.

However, as α increases further, the effects of ITP have an exaggerated effect on the model. From Eq. 21, as $P_{th}(t)$ (ITP) rises to the point where it begins to equal $P_{vc}(t)$, if $P_{vc}(t)$ does not increase, the stressed blood volume decreases until $P_{th}(t) = P_{vc}(t)$, at which point the stressed blood volume in the vena would become 0, preventing flow through the vena cava. The model's only means to prevent this issue is to increase vena cava pressure to maintain enough flow to prevent an incorrect SV. As vena cava pressure increases to account for this issue, this increase also causes an increase in left ventricle diastolic pressure, causing model and measured dynamics to diverge.

The increase in left ventricle diastolic pressure also causes an increase in error of left ventricular pulse pressure. Although it is not used in the error function of the model, Figure 8 shows the effect alpha has on the pulse pressure. As the diastolic pressure increases, model pulse pressure diminishes relative to the measurements. For low values of α, the pulse pressure error remains relatively stable through all values of PEEP. However, as α is increased, the errors begin to rise with PEEP.

Despite model equations being theoretically correct, when $\alpha = 1$ and ITP is fully transmitted to the left ventricle and vena cava, model errors become large and vena cava and left ventricle diastolic pressure dynamics begin to diverge from measurements. As stated previously, this outcome is a result of the entire venous blood system being subjected to ITP, rather than just the intrathoracic veins. The optimum α value successfully compensates for this, and the model is able to accurately reproduce system dynamics at high PEEP levels, while also producing observed cardiopulmonary interactions.

As seen in Figures 7 and 6, the α parameter also allows the model to adapt not only to patient specific conditions, but also changing conditions for a given patient. At $10cmH_2O$, Pig 4 had an optimum $\alpha = 0.3$, while at PEEP $= 5cmH_2O$, the optimum $\alpha = 0.6$. This change demonstrates the models ability to adapt to patient-specific conditions without requiring extra measurements or detailed understanding of patient-specific changes in condition.

4.4 Limitations

The model used omits the right circulation. As discussed previously, the right circulation is largely affected by MV, and plays a large role in resultant cardiopulmonary interactions. By omitting the right circulation, these effects cannot be physiologically accurately accounted for. However, there is also no measurement information of the right circulation typically available in the ICU. A model attempting to identify right sided haemodynamic parameters would thus be infeasible for most ICU use. Furthermore, despite the omission of the right circulation, the model is able to accurately and reliably tracks measurements and identifies haemodynamic parameters, while also accounting for the cardiopulmonary effects observed in the measured data.

A further limitation of the model is its inability to separate intra- and extra- thoracic

venous chambers. With an intra- and extra- thoracic venous chamber, the effect of ITP could be modelled with greater physiological accuracy, potentially yielding better results. Since there is only one venous measurement available in an ICU setting, an additional chamber would not be identifiable. However, with the α parameter, the model is able to compensate for this effect, while maintaining identifiability, and reliably and accurately produce model outputs while also reproducing both measured and observed cardiopulmonary interactions.

5 Conclusions

The α parameter proved successful, and an optimal value of α was found for each pig. The optimal α resulted in lower model error, and stabler model dynamics which closer matched those of the measurements. The α parameter was also validated by analysis of left ventricle pulse pressure error, a metric not included in the error function of the model. As hypothesised, left ventricle diastolic pressure increased with α, causing the model pulse pressure to diverge from the measurements.

While limiting the applied ITP to the vena cava and left ventricle with the α parameter is not entirely physiologically accurate, it compensates for the exaggerated effect ITP has on the system, due to the model's inability to separate intra- and extra- thoracic venous chambers, and is thus a more accurate approach than the original model. The α parameter allows for the inclusion of cardiopulmonary interactions through ITP, while also retaining model reliability at high PEEP levels, which the original cardiopulmonary lacked.

Finally, the α parameter allows the model to adapt to patient specific factors governing cardiopulmonary interactions without requiring an exact knowledge of any underlying conditions. Cardiopulmonary interactions and the resultant effects on the CVS are highly unpredictable and highly patient specific, providing a highly challenging task for accurate modelling. The problem is stressed even further when faced with questions of identifiability, as is the case in the ICU, where measurement data is relatively scarce compared to the physiological dynamics. The α parameter gives the model the ability to dynamically adapt to patient-specific thoracic cavity and lung mechanic responses to changes in PEEP, as well as patient specific conditions, providing more accurate and reliable model outputs and identified haemodynamic parameters. The use of the dynamic α parameter thus results in a model with the potential to guide both fluid therapy, and optimum PEEP levels for MV.

The improved reliability of the model, while maintaining identifiability, makes it a strong candidate for usage in the ICU. The model could be used to assist clinicians in simultaneously guiding both fluid therapy and mechanical ventilation, which are usually optimised separately and have potentially detrimental effects on each other. Future work would see a full validation of the improved model using human data from Christchurch hospital. Upon successful validation, the model will undergo clinical trials in Christchurch hospital, for use as a fluid therapy and mechanical ventilation guidance tool.

6 Declaration of Funding

This research did not receive any specific grant from funding agencies in the public, commercial, or not-for-profit sectors.

References

[1] B. O'Gara, "Perioperative lung protective ventilation," *BMJ*, vol. 362, 2018.

[2] N. Soni and P. Williams, "Positive pressure ventilation: what is the real cost?" *BJA: British Journal of Anaesthesia*, vol. 101, no. 4, pp. 446–457, 2008.

[3] G. H. Fodor, S. Bayat, G. Albu, N. Lin, A. Baudat, J. Danis, F. Peták, and W. Habre, *Frontiers in Physiology*, vol. 10, 2019. [Online]. Available: https://www.frontiersin.org/article/10.3389/fphys.2019.00803

[4] M. Cove, M. Pinsky, and J. Marini, "Are we ready to think differently about setting peep?" *Critical Care*, vol. 26, p. 222, 2022.

[5] Y. S. Chiew, J. G. Chase, G. M. Shaw, A. Sundareson, and T. Desaive, "Model-based peep optimisation in mechanical ventilation," *BioMedical Engineering Online*, vol. 10, 2011.

[6] V. J. Major, Y. S. Chiew, G. M. Shaw, and J. G. Chase, "Biomedical engineer's guide to the clinical aspects of intensive care mechanical ventilation," *Biomed Eng Online*, vol. 17, no. 1, 2018.

[7] A. C. Guyton and J. E. Hall, *Textbook of Medical Physiology*, 11th ed. Elsevier Saunders, 2006.

[8] A. Y. Denault, J. Gorcsan, and M. R. Pinsky, "Dynamic effects of positive-pressure ventilation on canine left ventricular pressure-volume relations," *Journal of Applied Physiology*, vol. 91, no. 1, pp. 298–308, 2001.

[9] S. Schuster, R. Erbel, L. S. Weilemann, W. Lu, B. Henkel, S. Wellek, H. Schinzel, and J. Meyer, "Hemodynamics during peep ventilation in patients with severe left ventricular failure studied by transesophageal echocardiography," *Chest*, vol. 97, no. 5, pp. 1181–1189, 1990.

[10] J. J. Maas, M. R. Pinsky, L. P. Aarts, and J. R. Jansen, "Bedside assessment of total systemic vascular compliance, stressed volume, and cardiac function curves in intensive care unit patients." *Anesthesia & Analgesia*, vol. 115, no. 4, pp. 880–887, 2021.

[11] T. Desaive, O. Horikawa, J. P. Ortiz, and J. G. Chase, "Model-based management of cardiovascular failure: Where medicine and control systems converge," *Annual Reviews in Control*, vol. 48, pp. 383–391, 2019.

[12] J. G. Chase, J.-C. Preiser, J. L. Dickson, A. Pironet, Y. S. Chiew, C. G. Pretty, G. M. Shaw, B. Benyo, K. Moeller, S. Safaei, M. Tawhai, P. Hunter, and T. Desaive, "Next-generation, personalised, model-based critical care medicine: a state-of-the art review of in silico virtual patient models, methods, and cohorts, and how to validation them," *BioMedical Engineering Online*, vol. 17, pp. 1–29, 2018.

[13] L. Murphy, S. Davidson, J. G. Chase, J. L. Knopp, T. Zhou, and T. Desaive, "Patient-specific monitoring and trend analysis of model-based markers of fluid responsiveness in sepsis: A proof-of-concept animal study." *Ann Biomed Eng*, vol. 48, pp. 682–694, 2020.

[14] J. Cushway, L. Murphy, J. G. Chase, G. M. Shaw, and T. Desaive, "Physiological trend analysis of a novel cardio-pulmonary model during a preload reduction manoeuvre," *Computer Methods and Programs in Biomedicine*, vol. 220, p. 106819, 2022.

[15] S. de Bournonville, A. Pironet, C. Pretty, J. G. Chase, and T. Desaive, "Parameter estimation in a minimal model of cardio-pulmonary interactions," *Mathematical Biosciences*, vol. 313, pp. 81–94, 2019.

[16] A. Pironet, P. C. Dauby, J. G. Chase, S. Kamoi, N. Janssen, P. Morimont, B. Lambermont, and T. Desaive, "Model-based stressed blood volume is an

index of fluid responsiveness," *IFAC-PapersOnLine*, vol. 48, no. 20, pp. 291–296, 2015, 9th IFAC Symposium on Biological and Medical Systems BMS 2015.

[17] B. W. Smith, J. Chase, R. I. Nokes, G. M. Shaw, and G. Wake, "Minimal haemodynamic system model including ventricular interaction and valve dynamics," *Medical Engineering & Physics*, vol. 26, no. 2, pp. 131–139, 2004.

[18] S. Safaei, C. P. Bradley, V. Suresh, K. Mithraratne, A. Muller, H. Ho, D. Ladd, L. R. Hellevik, S. W. Omholt, J. G. Chase, L. O. Müller, S. M. Watanabe, P. J. Blanco, B. de Bono, and P. J. Hunter, "Roadmap for cardiovascular circulation model," *The Journal of Physiology*, vol. 594, no. 23, pp. 6909–6928, 2016.

[19] P. J. Hunter and N. P. Smith, "The cardiac physiome project," *The Journal of Physiology*, vol. 594, no. 23, p. 6815–6816, 2016.

[20] B. W. Smith, S. Andreassen, G. M. Shaw, P. L. Jensen, S. E. Rees, and J. G. Chase, "Simulation of cardiovascular system diseases by including the autonomic nervous system into a minimal model," *Computer Methods and Programs in Biomedicine*, vol. 86, no. 2, pp. 153–160, 2007.

[21] A. Hobiny and I. Abbas, "Thermal response of cylindrical tissue induced by laser irradiation with experimental study," *International Journal of Numerical Methods for Heat & Fluid Flow*, vol. 22, no. 8, pp. 4013–4023, 2020.

[22] R. Beyar and Y. Goldstein, "Model studies of the effects of the thoracic pressure on the circulation," *Annals of Biomedical Engineering*, vol. 15, pp. 373–383, 1987.

[23] R. Beyar, H. R. Halperin, J. E. Tsitlik, A. D. Guerci, D. Kass, M. L. Weisfeldt, and N. C. Chandra, "Circulatory assistance by intrathoracic pressure variations: optimization and mechanisms studied by a mathematical model in relation to experimental data." *Circulation Research*, vol. 64, no. 4, pp. 703–720, 1989.

[24] R. Beyar, M. J. Hausknecht, H. R. Halperin, F. C. P. Yin, and M. L. Weisfeldt, "Interaction between cardiac chambers and thoracic pressure in intact circula-

tion," *American Journal of Physiology-Heart and Circulatory Physiology*, vol. 253, no. 5, pp. H1240–H1252, 1987.

[25] M. R. Pinsky, "The effects of mechanical ventilation on the cardiovascular system," *Critical Care Clinics*, vol. 6, no. 3, pp. 663–678, 1990, mechanical Ventilation.

[26] L. Gattinoni and J. J. Marini, "In search of the holy grail: identifying the best peep in ventilated patients," *Intensive Care Medicine*, 2022.

[27] J. L. Knopp, J. G. Chase, K. T. Kim, and G. M. Shaw, "Model-based estimation of negative inspiratory driving pressure in patients receiving invasive nava mechanical ventilation," *Computer Methods and Programs in Biomedicine*, vol. 208, p. 106300, 2021.

[28] J. H. T. Bates, *Lung mechanics: an inverse modeling approach*. Cambridge University Press, 2009.

[29] A. Baydur, "Monitoring lung mechanics," *Chest*, vol. 121, pp. 324–326, 2002.

[30] S. E. Morton, J. L. Knopp, J. G. Chase, P. Docherty, S. L. Howe, K. Möller, G. M. Shaw, and M. Tawhai, "Optimising mechanical ventilation through model-based methods and automation," *Annual Reviews in Control*, vol. 48, pp. 369–382, 2019.

[31] Y. S. Chiew, J. G. Chase, B. Lambermont, N. Janssen, C. Schranz, K. Moeller, G. M. Shaw, and T. Desaive, "Physiological relevance and performance of a minimal lung model – an experimental study in healthy and acute respiratory distress syndrome model piglets," *BMC Pulmonary Medicine*, vol. 12, 2012.

[32] A. Pironet, P. D. Docherty, P. C. Dauby, J. G. Chase, and T. Desaive, "Practical identifiability analysis of a minimal cardiovascular system model," *Computer Methods and Programs in Biomedicine*, vol. 171, pp. 53–65, 2019.

[33] H. Suga, K. Sagawa, and A. A. Shoukas, "Load independence of the instantaneous pressure-volume ratio of the canine left ventricle and effects of epinephrine and heart rate on the ratio," *Circulation Research*, vol. 32, no. 3, pp. 314–322, 1973.

[34] S. Davidson, C. Prett, A. Pironet, S. Kamoi, J. Balmer, T. Desaive, and J. G. Chase, "Minimally invasive, patient specific, beat-by-beat estimation of left ventricular time varying elastance," *BioMedical Engineering OnLine*, vol. 16, no. 42, 2017.

[35] A. I. Katz, Y. Chen, and A. H. Moreno, "Flow through a collapsible tube: Experimental analysis and mathematical model," *Biophysical Journal*, vol. 9, no. 10, pp. 1261–1279, 1969.

[36] R. A. Bronicki and N. G. Anas, "In search of the holy grail: identifying the best peep in ventilated patients," *Pediatric Critical Care Medicine*, vol. 10, no. 3, pp. 313–322, 2009.

[37] J. Teboul, W. Zapol, C. Brun-Buisson, F. Abrouk, A. Rauss, and F. Lemaire, "A comparison of pulmonary artery occlusion pressure and left ventricular end-diastolic pressure during mechanical ventilation with peep in patients with severe ards," *Anesthesiology*, vol. 70, no. 2, p. 261—266, February 1989.

[38] F. Jardin, J.-C. Farcot, L. Boisante, N. Curien, A. Margairaz, and J.-P. Bourdarias, "Influence of positive end-expiratory pressure on left ventricular performance," *New England Journal of Medicine*, vol. 304, no. 7, pp. 387–392, 1981.

[39] A. Pironet, P. C. Dauby, J. G. Chase, P. D. Docherty, J. A. Revie, and T. Desaive, "Structural identifiability analysis of a cardiovascular system model," *Medical Engineering & Physics*, vol. 38, no. 5, pp. 433–441, 2016.

[40] A. Pironet, "Model-based prediction of the response to vascular filling therapy," 2016.

[41] R. Smith, A. Rolfe, C. Cameron, G. M. Shaw, J. G. Chase, and C. G. Pretty, "Low cost circulatory pressure acquisition and fluid infusion rate measurement system for clinical research." *HardwareX*, p. e00318, 2022.

[42] S. Audoly, L. D'Angio, M. Saccomani, and C. Cobelli, "Global identifiability of linear compartmental models-a computer algebra algorithm," *IEEE Transactions on Biomedical Engineering*, vol. 45, no. 1, pp. 36–47, 1998.

[43] S. Audoly, G. Bellu, L. D'Angio, M. Saccomani, and C. Cobelli, "Global identifiability of nonlinear models of biological systems," *IEEE Transactions on Biomedical Engineering*, vol. 48, no. 1, pp. 55–65, 2001.

[44] A. J. Buda, M. R. Pinsky, J. Neil B. Ingels, G. T. Daughters, E. B. Stinson, and E. L. Alderman, "Effect of intrathoracic pressure on left ventricular performance," *N Engl J Med*, vol. 301, pp. 453–459, 1979, mechanical Ventilation.

[45] M. R. Pinsky, J.-M. Desmet, and J. L. Vincent, "Effect of positive end-expiratory pressure on right ventricular function in humans," *American Review of Respiratory Disease*, vol. 146, no. 3, 1992.

[46] S. S. Mahmood and M. R. Pinsky., "Heart-lung interactions during mechanical ventilation: the basics." *Annals of translational medicine*, vol. 6, no. 18, 2018.

[47] M. R. Grübler, O. Wigger, B. David, and S. Bloechlinger, "Basic concepts of heart-lung interactions during mechanical ventilation," *Swiss Medical Weekly*, vol. 147, 2017.

[48] S. Magder, A. Malhotra, K. A. Hibbert, and C. C. Hardin, *Cardiopulmonary Monitoring: Basic Physiology, Tools, and Bedside Management for the Critically Ill*. Springer, 2021.

[49] Q. Sun, J. G. Chase, C. Zhou, M. H. Tawhai, J. L. Knopp, K. Möller, and G. M. Shaw, "Over-distension prediction via hysteresis loop analysis and patient-specific basis functions in a virtual patient model," *Computers*

in Biology and Medicine, vol. 141, p. 105022, 2022. [Online]. Available: https://www.sciencedirect.com/science/article/pii/S0010482521008167

[50] C. Zhou, J. G. Chase, J. Knopp, Q. Sun, M. Tawhai, K. Möller, S. J. Heines, D. C. Bergmans, G. M. Shaw, and T. Desaive, "Virtual patients for mechanical ventilation in the intensive care unit," *Computer Methods and Programs in Biomedicine*, vol. 199, p. 105912, 2021.

[51] M. R. Pinsky, "Cardiopulmonary interactions: Physiologic basis and clinical applications," *Annals of the American Thoracic Society*, vol. 15, pp. S45–S48, 2018.

[52] J. Woods, P. Monteiro, and A. Rhodes, "Right ventricular dysfunction," *Current Opinion in Critical Care*, vol. 13, no. 5, pp. 532–540, 2007.

[53] V. Zochios, K. Parhar, W. Tunnicliffe, A. Roscoe, and F. Gao, "The right ventricle in ards," *Chest*, vol. 152, no. 1, pp. 181–193, 2017.